Efficient High-Energy Photon Production in the Supercritical QED Regime

Matteo Tamburini[1,*] and Sebastian Meuren[2,3,†]

[1] *Max-Planck-Institut für Kernphysik, Saupfercheckweg 1, D-69117 Heidelberg, Germany*
[2] *Stanford PULSE Institute, SLAC National Accelerator Laboratory, Menlo Park, CA 94025*
[3] *Department of Astrophysical Sciences, Princeton University, Princeton, NJ 08544*

(Dated: December 16, 2019)

When dense high-energy lepton bunches collide, the beam particles can experience a rest-frame field which greatly exceeds the QED critical one. Here it is demonstrated that beamstrahlung efficiently converts lepton energy to high-energy photons in this so-called supercritical QED regime, as the single-photon emission spectrum exhibits a pronounced peak close to the initial lepton energy. It is also shown that the observation of this high-energy peak in the photon spectrum requires to mitigate multiple photon emissions during the interaction. Otherwise, the photon recoil induces strong correlations between subsequent emissions which soften the photon spectrum and suppress the peak. The high-energy peak in the photon spectrum constitutes a unique observable of photon emission in the supercritical QED regime and paves the way to a laserless gamma-gamma collider based on electron-electron collisions.

A future (multi-) TeV lepton collider has to be linear in order to mitigate energy losses via synchrotron radiation. As two colliding bunches cross only once in a linear collider, extremely high particle densities need to be created at the interaction point in order to achieve the luminosities required to search for physics beyond the standard model [1–3]. As a result, beamstrahlung energy losses become a decisive design concern [4–7].

Beamstrahlung is primarily characterized by the quantum parameter $\chi = \Upsilon = F^*/F_{\rm cr}$, where F^* denotes the electric field in the rest frame of a beam particle and $F_{\rm cr} = m^2c^3/|e|\hbar \approx 1.3\times10^{18}\,\mathrm{V/m}$ is the QED critical (Schwinger) field ($F_{\rm cr}/c \approx 4.4\times10^9\,\mathrm{T}$). Classical electrodynamics is valid for $\chi \ll 1$, whereas strong-field quantum corrections become important if $\chi \gtrsim 1$ [8, 9].

In the regime $\chi \ll 1$ the recoil of each individual photon is small, such that the total radiated energy $\delta\varepsilon$ is the decisive quantity [6, 8]

$$\frac{\delta\varepsilon}{\varepsilon} \sim \alpha\chi^2\frac{\ell}{\gamma\lambda\!\!\!^{-}_c} \sim \frac{\gamma\lambda\!\!\!^{-}_c}{\ell}, \quad \chi \sim N\alpha\frac{\lambda\!\!\!^{-}_c}{\sigma}\frac{\gamma\lambda\!\!\!^{-}_c}{\ell}. \tag{1}$$

Here, ℓ denotes the longitudinal bunch length, σ its rms radius, N the total number of particles, $\gamma = \varepsilon/(mc^2)$ the relativistic Lorentz factor, $\lambda\!\!\!^{-}_c = \hbar/(mc) \approx 3.9\times10^{-13}\,\mathrm{m}$ the electron/positron Compton wavelength and $\alpha = e^2/(4\pi\epsilon_0\hbar c) \approx 1/137$ the fine-structure constant. As a consequence, current collider designs such as ILC and CLIC [3] employ long bunches ($\gamma\lambda\!\!\!^{-}_c/\ell \ll 1$) in order to minimize $\delta\varepsilon$.

Recently, it was suggested in Ref. [10] that beamstrahlung could also be mitigated by operating in the supercritical quantum regime ($\chi \gg 1$). As a single photon emission on average induces a large recoil, the radiation probability W is the relevant quantity now [6, 8]

$$W \sim \alpha\chi^{2/3}[\ell/(\gamma\lambda\!\!\!^{-}_c)] \sim [\ell/(\gamma\lambda\!\!\!^{-}_c)]^{1/3}. \tag{2}$$

Correspondingly, in this regime it is beneficial to employ very dense and short bunches [$\ell/(\lambda\!\!\!^{-}_c\gamma) \ll 1$], which minimizes the radiation probability and increases the beam self-fields [see Eq. (1)]. Thus, a thorough understanding of QED in supercritical electromagnetic fields ($\chi \gg 1$) becomes important. Notably, the required technology to produce ultracompressed lepton beams exists [11].

Whereas the regime $\chi \lesssim 1$ is relatively well explored theoretically [8, 9] (see [12–14] for recent experiments), the supercritical QED regime $\chi \gg 1$ is still poorly understood. When $\alpha\chi^{2/3} \gtrsim 1$ ($\chi \gtrsim 10^3$) radiative corrections might become significant [8], and even a complete breakdown of perturbation theory has been conjectured [15, 16] (see also [17–19] for recent theoretical studies and [10, 20–23] for proposals to probe this regime experimentally). To circumvent theoretical uncertainties, we limit ourselves to $\chi \lesssim 100$ in the following.

Here, we show that qualitatively new features appear in the photon emission spectrum already with $\chi \gg 1$ but $\alpha\chi^{2/3} \ll 1$. In particular, we demonstrate that (i) for $\chi \gtrsim 16$ the single-photon emission spectrum exhibits a pronounced peak close to the initial electron energy, such that the probability for an electron to emit a single photon carrying almost all the electron energy strongly increases, (ii) the single-emission photon spectrum can be measured in asymmetric electron-electron beam collisions, (iii) when multiple photon emissions become dominant, the high-energy peak in the total and, remarkably, even in the single-photon emission spectrum vanishes. Thus, efficient high-energy photon production requires to operate in a regime where on the one hand most electrons emit – favoring a long interaction time – and on the other hand multiple emissions by the same electron are subdominant, which favors a short interaction time.

Notably, the height of the peak in the spectrum provides quantitative information about the average χ experienced by the beam particles during the interaction. In addition to its intrinsic interest, as it provides an observable of the supercritical QED regime, these findings also pave the way to an efficient gamma-gamma collider based on beamstrahlung. As Compton backscattering becomes

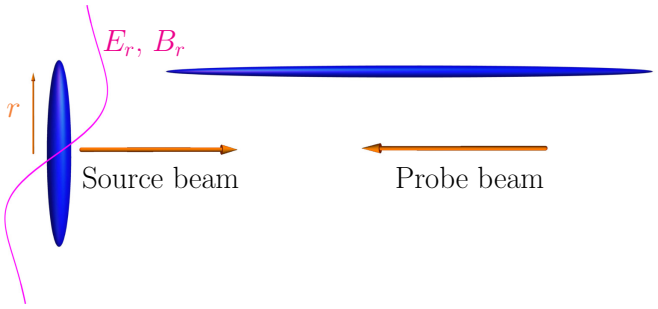

FIG. 1. Schematic setup. A pancake shape dense source beam collides with an elongated cigar shape low-density probe beam. The probe beam collides with a transverse impact parameter r, such that the source beam electric E_r and magnetic B_r fields approach their maximum.

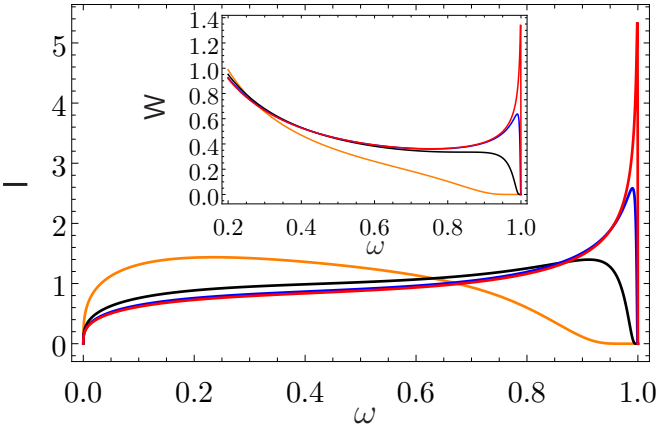

FIG. 2. Photon emission spectrum $\mathsf{I} = d^2I/dt\,d\omega(dI/dt)^{-1}$ and probability $\mathsf{W} = d^2W/dt\,d\omega(dW/dt)^{-1}$ (inset) for $\chi = 1.6$ (orange), $\chi = 16$ (black), $\chi = 160$ (blue), and $\chi = 1600$ (red).

increasingly more challenging to realize with increasing center-of-mass energy [24, 25], beamstrahlung represents a very attractive source for high-energy photons [26, 27]. However, as the pronounced peak in the photon emission spectrum is a unique signature which occurs exclusively in the supercritical quantum regime ($\chi \gg 1$), the discussion presented here is qualitatively different from the previously considered regime $\chi \lesssim 1$ [26, 27].

In the following we consider an asymmetric electron-electron collider setup (see Fig. 1). A short dense pancake-shape electron "source" beam collides head-on with an elongated cigar-shape low-density but high-energy "probe" beam. As the electromagnetic field experienced by the probe beam particles changes significantly as a function of the impact parameter, the considered asymmetric setup avoids a trivial average over different values of χ, which is always present in symmetric collisions. In comparison with symmetric collisions the "source" beam provides the strong field, i.e., its longitudinal length (ℓ), transverse rms size (σ), and number of electrons (N) are relevant for calculating χ [see Eq. (1)]. On the other hand the high-energy "probe" beam provides the large gamma factor γ to boost the experienced rest frame field. In the following all source (probe) beam parameters are denoted with the subscript s (p).

Before considering a concrete choice of collider parameters, we analyze the single-photon emission probability. For convenience, we introduce the normalized photon energy $\omega = \varepsilon_\gamma/\varepsilon$, where ε is the initial energy of the emitting electron and ε_γ is the energy of the emitted photon. The differential radiation probability is given by [28]

$$\frac{d^2W}{dt\,d\omega} = \frac{\alpha}{\sqrt{3}\pi\tau_c\gamma}\left\{\left[2+\frac{\omega^2}{(1-\omega)}\right]\mathrm{K}_{2/3}\left[\frac{2\omega}{3\chi(1-\omega)}\right] - \int_{2\omega/[3\chi(1-\omega)]}^{\infty} dy\ \mathrm{K}_{1/3}(y)\right\}, \quad (3)$$

where $\tau_c = \hbar/(mc^2)$ is the Compton time and $\mathrm{K}_\nu(x)$ is the modified Bessel function of second kind [29]. Correspondingly, the emission rate is $dW/dt = \int_0^1 d\omega\, d^2W/dtd\omega$, while the normalized emitted power is $dI/dt = \int_0^1 d\omega\, d^2I/dt\,d\omega$, where $d^2I/dtd\omega = \omega d^2W/dtd\omega$.

A detailed analysis of Eq. (3) reveals a distinctive feature of the photon emission spectrum which occurs exclusively in the supercritical quantum regime. Whereas $d^2W/dtd\omega$ is a monotonically decreasing function of ω for $\chi \lesssim 16$, it develops a local minimum and maximum for $\chi \gtrsim 16$, which results in a peak close to $\omega = 1$ (see inset of Fig. 2 and Ref. [30]). The minimum and maximum are approximately located at

$$\begin{aligned} \omega_{\min} &\approx 0.754 + \frac{(15.7+0.146\chi)}{\chi^2}; \quad (\chi > 16), \\ \omega_{\max} &\approx 1 - \frac{(174+20\chi)}{15\chi^2}; \quad (\chi > 16). \end{aligned} \quad (4)$$

The height of the peak H is given by

$$H = \frac{(d^2W/dtd\omega)(\omega_{\max})}{(d^2W/dtd\omega)(\omega_{\min})} \approx \frac{1.315+0.315\chi}{\chi^{2/3}}, \quad (5)$$

and provides a unique physical observable of the average value of χ achieved during the interaction.

Figure 2 displays normalized emission spectrum and photon emission probability in four different regimes: (i) the critical regime ($\chi \sim 1$, orange line), (ii) transition between the critical and the supercritical regime ($\chi \sim 10$, black line), (iii) the supercritical regime ($\chi \sim 100$, blue line), and (iv) the fully nonperturbative regime ($\alpha\chi^{2/3} \sim 1$ red line). Whereas electrons still emit in a broad energy range for $\chi \sim 1$, a sharp peak close to the initial electron energy ($\omega \approx 1$) appears in the supercritical regime ($\chi > 16$). The probability of producing a photon with energy beyond $\omega_{\min}$ already exceeds 9% for $\chi > 60$, and basically saturates to approximately 11% for

$\chi \gtrsim 800$. However, the height of the peak monotonically increases with increasing χ, i.e., the quasimonochromatic features of the photon spectrum at $\omega \approx 1$ increasingly improve [see Eq. (5) and Fig. 2].

In order to quantitatively investigate the photon emission spectrum 3D Monte Carlo simulations of beam-beam collision were performed. The source beam has 10 GeV energy, 0.96 nC charge, $\ell_s = 100\,\mathrm{nm}$ bunch length (in the laboratory frame), and $\sigma_s = 300\,\mathrm{nm}$ transverse size. In the laboratory, a maximum electric (magnetic) field of $E_{\max} \approx 2.6 \times 10^{14}\,\mathrm{V/m}$ ($B_{\max} \approx 8.6 \times 10^5\,\mathrm{T}$) is achieved at an impact parameter of $r \approx 500\,\mathrm{nm}$. In the simulations a 3D analytical solution of Maxwell's equations was used for the electromagnetic fields of the source beam (see Supplemental Material). Note that the energy of the source beam is not relevant for attaining large χ_p, but its beam density is decisive. In practice, however, longitudinal beam compression becomes only feasible at sufficiently large gamma factors. The parameters here are comparable to those achievable at the FACET-II facility at SLAC [11].

The probe beam has 100 GeV energy with 100 MeV rms energy spread, 16 pC charge, $\ell_p = 300\,\mu\mathrm{m}$ bunch length, and $\sigma_p = 50\,\mathrm{nm}$ transverse size. As a result, the maximum electric (magnetic) field of the probe beam $E_{\max} \approx 8.7 \times 10^9\,\mathrm{V/m}$ ($B_{\max} \approx 29\,\mathrm{T}$) at $r \approx 80\,\mathrm{nm}$ is much weaker and its density is much lower than for the source beam. Thus, the source beam is basically unaffected by the interaction. Due to the finite transverse size of the probe beam χ_p ranges approximately from 75 to 77. For the above parameters the average emission probability per electron is approximately 0.12. Figure 3a reports the photon energy distribution for electrons which emitted *only one* (*two*) photon(s) during the interaction [orange (black) line] and the total photon distribution (blue line). Accordingly, the photon spectrum is dominated by single emissions while secondary and higher-order processes are suppressed (see also the inset of Fig. 4). The peak height H obtained from simulations (total spectrum, blue line) corresponds to $\chi_p \approx 69$ if Eq. (5) is employed. This value is within the 10% error margin which we expect due to the presence of multiple emissions. In fact, H provides a lower bound to χ_p, which tends to the actual value in the limit of single emission.

Next, we consider the same parameters as above but increase (decrease) the source beam length (transverse size) by a factor of 25, i.e., employ $\ell_s = 2500\,\mathrm{nm}$ and $\sigma_s = 12\,\mathrm{nm}$. This scaling leaves the peak field invariant [see Eq. (1)], which is now reached at an impact parameter of $r = 20\,\mathrm{nm}$. To keep the variation of χ_p comparable to the first simulation, we also reduce the transverse size of the probe beam to $\sigma_p = 2\,\mathrm{nm}$. As a result, the average number of photon emissions per electron increases to approximately 3.0 (see Fig. 3b and Fig. 4). In contrast to the previous simulation, the spectrum no longer exhibits a peak.

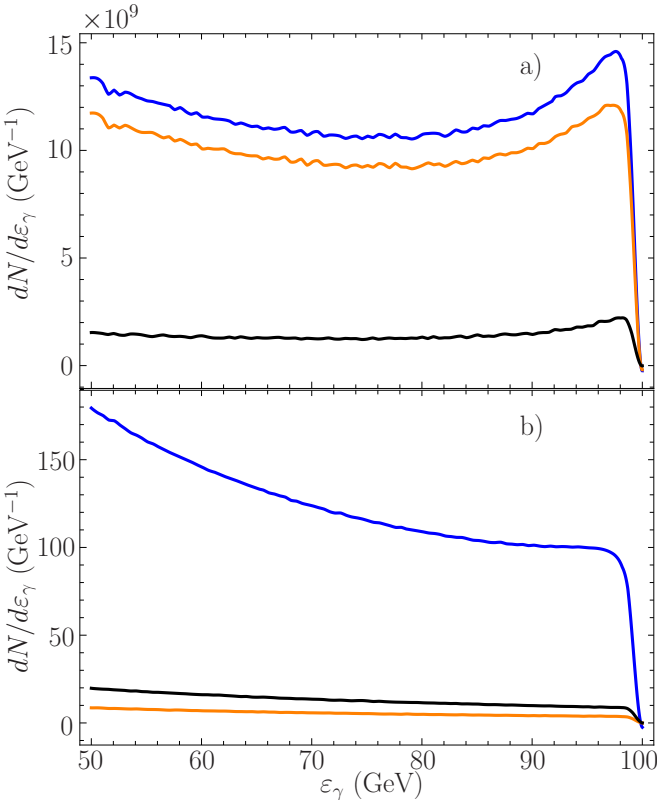

FIG. 3. Photon emission probability. The solid orange, black and blue lines report photons that originate from electrons that emitted only once, only twice, and all final photons, respectively. **a)** short interaction time ($\ell_s = 100\,\mathrm{nm}$), single emissions dominant **b)** long interaction time ($\ell_s = 2500\,\mathrm{nm}$, multiple emissions dominant. See the main text for further details.

In order to explain this transition, we assume that a probe particle experiences the supercritical quantum regime ($\chi_p \gg 1$). As shown in Fig. 2, it is likely that this particle emits a hard photon with $\omega \approx 1$. Due to the large recoil, the probe particle has a much lower energy $\varepsilon' = \varepsilon(1-\omega)$ after the emission. In the regime $\chi_p \gg 1$, the scaling $W_p \sim [\ell_s/(\lambda_c \gamma_p)]^{1/3}$ [see Eq. (2)] implies that a particle with lower energy has an increased radiation probability. Therefore, the emission of a hard photon ($\omega \approx 1$) increases the probability to emit a second photon, which is on average much softer. On the contrary, the emission of a soft photon ($\omega \ll 1$) is less likely followed by a second emission. As a consequence, we expect the peak to vanish in the total photon spectrum when multiphoton emissions are dominant. Remarkably, the peak disappears also in the one-photon emission spectrum, which is naively not expected based on perturbation theory (see below).

In the following the photon emission distribution is calculated analytically. Assuming that the local-constant-field approximation (LCFA) holds, the single-photon emission probability given in Eq. (3) is always applicable

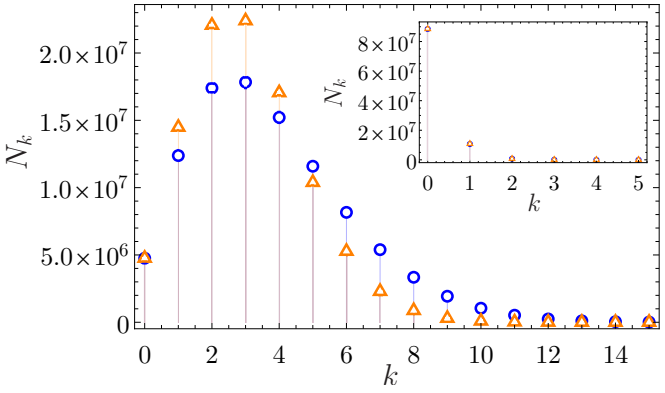

FIG. 4. Number of emitted photons N_k as function of the number of photon emissions k. Blue circles report the simulation results, orange triangles the Poisson prediction. **Main plot**: $\ell_s = 2500\,\mathrm{nm}$, **Inset**: $\ell_s = 100\,\mathrm{nm}$.

for sufficiently small time intervals dt. Thus, the probability $S(t,t';\varepsilon)$ that an electron with energy ε does *not* emit a photon during the time interval $[t,t']$ is given by (see Supplemental Material)

$$S(t,t';\varepsilon) = \exp\left[-\int_{t'}^{t} d\tau\,\frac{dW}{d\tau}(\varepsilon,\tau)\right]. \tag{6}$$

Correspondingly, the electron "decays" exponentially, with a radiative lifetime given by the total emission probability per unit time $dW(\varepsilon,t)/dt = \int_0^\varepsilon d\varepsilon'\, d^2W(\varepsilon',\varepsilon,t)/dt\,d\varepsilon'$. As $\varepsilon' = \varepsilon(1-\omega)$, the quantities $d^2W/dtd\varepsilon'$ and $d^2W/dtd\omega$ are trivially related [see Eq. (3)]. Note that in ab-initio S-matrix–based calculations of the photon emission probability the decay exponent $S(t,t';\varepsilon)$ appears self-consistently once radiative corrections to the electron states are properly taken into account [31].

From $S(t,t';\varepsilon)$, the probability $(dP_1/d\varepsilon')(\varepsilon',t)$ that an electron has an energy within $[\varepsilon',\varepsilon'+d\varepsilon']$ at time t after radiating exactly one photon is

$$\frac{dP_1}{d\varepsilon'}(\varepsilon',t) = \int_{-\infty}^{t} d\tau\, S(t,\tau;\varepsilon') \times \frac{d^2W}{d\tau\,d\varepsilon'}(\varepsilon',\varepsilon_i,\tau) S(\tau,-\infty;\varepsilon_i). \tag{7}$$

Here and in the following, ε_i denotes the initial electron energy, we implicitly assume that the work performed by the external field is negligible compared to the electron energy, and $\chi(t)$ is obtained from the electron trajectory. Equation 7 explains the suppression of the peak even in the one-photon emission spectrum when multiple emissions become dominant (see Fig. 3). In fact, in the regime $\chi \gg 1$ substantial recoil is likely, which implies $\varepsilon' \ll \varepsilon_i$. Correspondingly, the decay exponent after the emission $S(\infty,\tau;\varepsilon')$ is substantially smaller than it would be with negligible recoil $S(\infty,\tau;\varepsilon' \approx \varepsilon_i)$, i.e., the electron "radiative lifetime" substantially decreases after the emission. Therefore, the high-energy part of the spectrum $\omega = 1-\varepsilon'/\varepsilon_i \approx 1$ is, for sufficiently long interaction time, suppressed. Consequently, even the single-photon emission spectrum differs qualitatively from Eq. (3) (compare Fig. 3a and Fig. 3b). Note that for short interaction times $S(\infty,\tau;\varepsilon') \approx 1$, independently of the magnitude of the recoil [see Eq. (6)] and the spectrum coincides with Eq. (3).

Equation 8 can be easily generalized to n photon emissions (see Supplemental Material for further details)

$$\frac{dP_n}{d\varepsilon'}(\varepsilon',t) = \int_{-\infty}^{t} d\tau\, S(t,\tau;\varepsilon') \times \int_{\varepsilon'}^{\varepsilon_i} d\varepsilon\,\frac{d^2W}{d\tau\,d\varepsilon'}(\varepsilon',\varepsilon,\tau)\frac{dP_{n-1}}{d\varepsilon}(\varepsilon,\tau). \tag{8}$$

In Eqs. (7), (8) we implicitly assumed that the local radiation probability $(d^2W/d\tau d\varepsilon')(\varepsilon',\varepsilon,\tau)$ depends only on the time τ at which the photon is emitted and on the electron instantaneous energy ε. However, the position of the electron and thus the instantaneous field strength depends, in general, on the full history of previous emissions and not just on τ and ε. Assuming that the particle is ultrarelativistic and that the background field is sufficiently homogeneous in transverse direction, this is a reasonable approximation. This assumption holds exactly for plane-wave background fields, if the laser phase is used as generalized time and the light-front momentum as generalized energy coordinate.

Finally, we are interested in the asymptotic probabilities P_n than an electron has emitted exactly n photons during the interaction

$$P_n = P_n(\infty), \quad P_n(t) = \int_0^{\varepsilon_i} d\varepsilon'\,\frac{dP_n}{d\varepsilon'}(\varepsilon',t), \tag{9}$$

with $P_0(t) = S(t,-\infty;\varepsilon_i)$. In the classical limit ($\chi \ll 1$) the photon recoil is negligible and $S(t,\tau;\varepsilon)S(\tau,t';\varepsilon) = S(t,t';\varepsilon)$, such that the number of emitted photons P_n follows a Poissonian distribution [32–34]

$$P_n = \frac{\mathcal{W}^n}{n!}\exp(-\mathcal{W}), \quad \langle n\rangle = \sum_{n=0}^{\infty} nP_n = \mathcal{W}. \tag{10}$$

Here, the decay exponent $\mathcal{W} = \int_{-\infty}^{+\infty} d\tau\,(dW/d\tau)(\varepsilon_i,\tau)$ factorizes, is independent of the number of emitted photons and constant across the spectrum. This is in sharp contrast to the $\chi \gg 1$ regime, where $S(t,\tau;\varepsilon')S(\tau,t';\varepsilon_i) \neq S(t,t';\varepsilon_i)$ and the decay exponent is strongly dependent on the energy of each emitted photon. Note that in an S-matrix–based derivation of Eq. (10) the appearance of the nonperturbative decay exponent is a consequence of radiative corrections [32, 33].

In Fig. 4 the simulated distribution (blue circles) is compared to the Poissonian prediction (orange triangles).

For short interaction times (inset of Fig. 4) P_0 is dominant, and the Poissonian approximation is valid. However, when $P_{n>0}$ is dominant and $\chi \gg 1$, substantial deviations are found (see the main plot of Fig. 4).

In summary, we have shown that the beamstrahlung spectrum exhibits a peak at high energies in the supercritical quantum regime ($\chi \gg 1$; see Fig. 2) and that this peak is observable in asymmetric electron-electron collisions (see Fig. 3a). Moreover, we have shown that due to the presence of strong correlations, this peak vanishes in a regime where multiphoton emissions become dominant (see Fig. 3b). In particular, we have found that radiation reaction changes even the single-photon emission spectrum qualitatively in this regime. The recoil-induced correlations between different photon emissions manifest themselves in a photon statistic which significantly deviates from a Poissonian distribution (see Fig. 4). The reported observations imply that a photon-photon collider based on beamstrahlung has to balance between a large conversion efficiency (favoring a long interaction time) and a sufficiently good suppression of soft photons (favoring a short interaction time).

The authors would like to thank Fabrizio Del Gaudio, Antonino Di Piazza, Gerald Dunne, Nathaniel Fisch, Thomas Grismayer, Christoph Keitel, Michael Peskin, David Reis, Luís Silva, Glen White, Vitaly Yakimenko, and all participants of the 2019 SLAC workshop *"Physics Opportunities at a Lepton Collider in the Fully Nonperturbative QED Regime"* for stimulating discussions. At SLAC, SM was supported by the U.S. Department of Energy under contract number DE-AC02-76SF00515. At Princeton, SM received funding from the Deutsche Forschungsgemeinschaft (DFG, German Research Foundation) under Grant No. 361969338.

MT discovered that a peak appears in the photon emission probability in the supercritical QED regime for $\chi \gtrsim 16$ and studied its properties in 2014 and, in particular, obtained Eqs. (4)-(5) of the main text, Eqs. (1)-(2c) of the Supplemental Material, and performed the statistical analysis on the photon emission number distribution. SM independently considered the influence of the radiative decay on the single-photon emission spectrum for $\chi < 10$, joined the project in 2016, and pointed out the peak suppression in the multiphoton regime. The manuscript was written equally by both authors, with simulations and figures by MT.

* matteo.tamburini@mpi-hd.mpg.de
† smeuren@stanford.edu

[1] M. Tanabashi et al. (Particle Data Group), Phys. Rev. D **98**, 030001 (2018).
[2] B. Badelek et al., Int. J. Mod. Phys. A **19**, 5097 (2004).
[3] P. Lebrun, L. Linssen, A. Lucaci-Timoce, D. Schulte, F. Simon, S. Stapnes, N. Toge, H. Weerts, and J. Wells, *The CLIC programme: Towards a staged e^+e linear collider exploring the terascale: CLIC conceptual design report*, CERN Yellow Reports: Monographs (CERN, Geneva, 2012) comments: 84 pages, published as CERN Yellow Report https://cdsweb.cern.ch/record/1475225.
[4] R. J. Noble, Nucl. Inst. Meth. Phys. Res. A **256**, 427 (1987).
[5] P. Chen, Phys. Rev. D **46**, 1186 (1992).
[6] K. Yokoya and P. Chen, Frontiers of Particle Beams: Intensity Limitations , 415 (1992).
[7] J. Esberg, U. Uggerhøj, B. Dalena, and D. Schulte, Phys. Rev. ST Accel. Beams **17**, 051003 (2014).
[8] V. I. Ritus, J. Russ. Laser Res. **6**, 497 (1985).
[9] A. Di Piazza, C. Müller, K. Z. Hatsagortsyan, and C. H. Keitel, Rev. Mod. Phys. **84**, 1177 (2012).
[10] V. Yakimenko, S. Meuren, F. Del Gaudio, C. Baumann, A. Fedotov, F. Fiuza, T. Grismayer, M. J. Hogan, A. Pukhov, L. O. Silva, and G. White, Phys. Rev. Lett. **122**, 190404 (2019).
[11] G. White and V. Yakimenko, "Ultra-short-z linear collider parameters," (2018), arXiv:1811.11782 [physics.acc-ph].
[12] J. M. Cole, K. T. Behm, E. Gerstmayr, T. G. Blackburn, J. C. Wood, C. D. Baird, M. J. Duff, C. Harvey, A. Ilderton, A. S. Joglekar, K. Krushelnick, S. Kuschel, M. Marklund, P. McKenna, C. D. Murphy, K. Poder, C. P. Ridgers, G. M. Samarin, G. Sarri, D. R. Symes, A. G. R. Thomas, J. Warwick, M. Zepf, Z. Najmudin, and S. P. D. Mangles, Phys. Rev. X **8**, 011020 (2018).
[13] K. Poder, M. Tamburini, G. Sarri, A. Di Piazza, S. Kuschel, C. D. Baird, K. Behm, S. Bohlen, J. M. Cole, D. J. Corvan, M. Duff, E. Gerstmayr, C. H. Keitel, K. Krushelnick, S. P. D. Mangles, P. McKenna, C. D. Murphy, Z. Najmudin, C. P. Ridgers, G. M. Samarin, D. R. Symes, A. G. R. Thomas, J. Warwick, and M. Zepf, Phys. Rev. X **8**, 031004 (2018).
[14] T. N. Wistisen, A. Di Piazza, H. V. Knudsen, and U. I. Uggerhøj, Nat. Commun. **9**, 795 (2018).
[15] V. I. Ritus, Sov. Phys. JETP **30**, 1181 (1970).
[16] N. B. Narozhny, Phys. Rev. D **21**, 1176 (1980).
[17] A. Fedotov, J. Phys.: Conf. Ser. **826**, 012027 (2017).
[18] T. Podszus and A. Di Piazza, Phys. Rev. D **99**, 076004 (2019).
[19] A. Ilderton, Phys. Rev. D **99**, 085002 (2019).
[20] T. G. Blackburn, A. Ilderton, M. Marklund, and C. P. Ridgers, New J. Phys. **21**, 053040 (2019).
[21] C. Baumann, E. N. Nerush, A. Pukhov, and I. Y. Kostyukov, Sci. Rep. **9**, 9407 (2019).
[22] C. Baumann and A. Pukhov, Plasma Phys. Control. Fusion **61**, 074010 (2019).
[23] A. Di Piazza, T. N. Wistisen, M. Tamburini, and U. I. Uggerhøj, (2019), arXiv:1911.04749.
[24] V. Telnov, Nucl. Inst. Meth. Phys. Res. A **294**, 72 (1990).
[25] J. Gronberg, Reviews of Accelerator Science and Technology **07**, 161 (2014).
[26] R. Blankenbecler and S. D. Drell, Phys. Rev. Lett. **61**, 2324 (1988).
[27] F. Del Gaudio, T. Grismayer, R. A. Fonseca, W. B. Mori, and L. O. Silva, Phys. Rev. Accel. Beams **22**, 023402 (2019).
[28] V. N. Baier, V. M. Katkov, and V. M. Strakhovenko, *Electromagnetic Processes at High Energies in Oriented Single Crystals* (World Scientific, Singapore, 1998).
[29] F. W. J. Olver, D. W. Lozier, R. F. Boisvert, and C. W.

Clark, eds., *NIST handbook of mathematical functions* (Cambridge University Press, Cambridge, 2010).
[30] S. S. Bulanov, C. B. Schroeder, E. Esarey, and W. P. Leemans, Phys. Rev. A **87**, 062110 (2013).
[31] S. Meuren and A. Di Piazza, Phys. Rev. Lett. **107**, 260401 (2011).
[32] C. Itzykson and J. B. Zuber, *Quantum field theory* (Dover Publications, 2005).
[33] R. J. Glauber, Physical Review **84**, 395 (1951).
[34] A. Di Piazza, K. Z. Hatsagortsyan, and C. H. Keitel, Phys. Rev. Lett. **105**, 220403 (2010).